Simulation Model with an Optimal Operation Strategy for a Hybrid Train Powered by a Battery and a Fuel Cell

Cem Ünlübayir
Institute for Power Electronics and Electrical Drives (ISEA ESS)
RWTH Aachen University
Aachen, Germany
cem.uenluebayir@isea.rwth-aachen.de

Thomas Nemeth
Institute for Power Electronics and Electrical Drives (ISEA ESS)
RWTH Aachen University
Aachen, Germany
thomas.nemeth@isea.rwth-aachen.de

Fabian Meishner
Institute for Power Electronics and Electrical Drives (ISEA ESS)
RWTH Aachen University
Aachen, Germany
fabian.meishner@isea.rwth-aachen.de

Hujun Peng
Institute of Electrical Machines (IEM)
RWTH Aachen University
Aachen, Germany
hujun.peng@iem.rwth-aachen.de

Kai Deng
Institute of Electrical Machines (IEM)
RWTH Aachen University
Aachen, Germany
kai.deng@iem.rwth-aachen.de

Dirk Uwe Sauer
Institute for Power Electronics and Electrical Drives (ISEA ESS)
RWTH Aachen University
Aachen, Germany
dirkuwe.sauer@isea.rwth-aachen.de

***Abstract*—The electrification of railroad transportation without overhead lines is of particular interest with regard to the reduction of air pollutants. An electrified hybrid train powered by a battery and a fuel cell is a promising topology to replace trains running with diesel. An energy management strategy has to utilize the advantages of both components the best and reach the lowest possible costs. To find this strategy, we implemented a detailed simulation model of the hybrid train. We benchmarked a rule-based energy management strategy for the distribution of the load against a dynamic programming (DP) and a quadratic programming (QP) optimization approach. The results show that the utilization of an optimization approach can reduce the fuel economy of a drive cycle by more than one third.**

Keywords—fuel cell hybrid train, battery hybrid train, energy management, battery model, simulation, operation strategy

I. Introduction

With the ongoing decarbonisation of most transportation sectors, many nations have the goal to advance the electrification of their existing rail network. However, diesel trains are still frequently used in rail freight transport and in rail transport services. In Europe, for example, regional trains with diesel propulsion are still common because of a lack of affordable alternatives [1]. In 2017, circa 26 percent of all rail lines worldwide were electrified, i.e. equipped with an overhead contact line [2]. In 2016, 52.8 percent of all railway tracks in Germany were electrified, while the percentage of electrified railway lines in Europe amounts to 60 percent [1, 3]. A promising topology for trains operated in track sections without overhead lines is a parallel hybrid topology in which a fuel cell system and a battery system power the drive train. With its slow dynamic responsiveness, the fuel cell covers the basic demand for electrical power. The battery covers the dynamic requirements such as acceleration or recuperation [4]. The ability to recuperate braking energy is apart from the environmental aspect another advantage of electric trains over trains with diesel engines. If otherwise the fuel cell had to cover dynamic loads, it would leave its optimal operation point frequently. For the power distribution between the components, this inertia and the system boundaries of the components shall be considered. Within the framework of a research project, we investigate the technological feasibility of this hybrid train concept, implemented a comprehensive simulation model and aim to validate hardware components on a hardware-in-the-loop (HIL) test bench. The simulation model contains precise models of each power train component. In this model, an energy management unit (EMU) distributes the power between the battery system and the fuel cell system. In train operations, routes or speed profiles are typically predefined. This makes it possible for us to optimize the fuel economy for known drive cycles off-line beforehand.

There are a number of sources dealing with the modelling of hybrid vehicles and their operating or energy management strategies [5, 6, 7]. The goal of this research is to present different strategies for the power distribution and compare the operation strategies in terms of fuel economy. An on-line power distribution is compared to two off-line optimization approaches for the power distribution of the demanded load. One of the examined optimization approaches, dynamic programming (DP), is considered to find the optimal solution [8, 9]. However, it is shown that a quadratic programming (QP) optimization approach can reduce the costs of the examined drive cycle and the calculation time of the simulation significantly.

The target application of this simulation model is a hardware-in-the-loop (HIL) test bench, in which some of the hybrid train components are tested. The simulation model will be integrated into the control system of the test bench and perform energy management tasks.

In the following, the simulation model as well as the strategies are described in detail. In section III, the simulation results of the operation strategies are shown and discussed.

II. Technological Concept

A. The simulation model of the power train

Figure 1 shows the investigated power train concept for the hybrid train.

978-1-7281-0962-6/19/$31.00 ©2019 IEEE

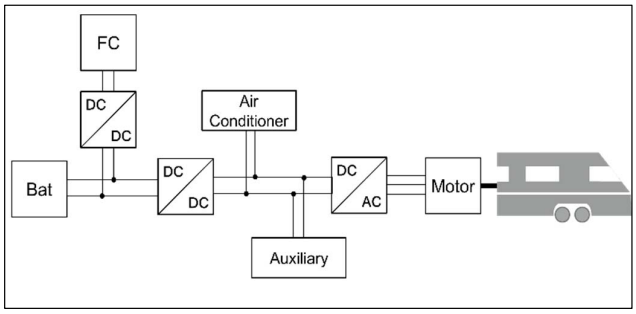

Figure 1: Power train topology with the battery (Bat) and the fuel cell (FC).

The examined hybrid train has two propulsion components:

- A battery system with a capacity of 200 kWh / 210 Ah using lithium-titanate (LTO) battery cells to guarantee high charge- and discharge currents to handle dynamic loads up to 1 MW. Tests conducted by our research group on the LTO-cells show that after cycling between 10 and 90 % state-of-charge (SoC) with 4400 equivalent full cycles, the battery has a remaining capacity of between 93 to 94 % of the initial capacity. The cycle tests were carried out with currents corresponding to the real train operation.
- A 200 kW proton-exchange membrane fuel cell system.

In addition to the propulsion components, the DC-DC converters are modelled as a look-up table with their efficiency at each operation point. Furthermore, an air conditioner unit and an auxiliary unit are considered as loads in the simulation model. The simulation model runs on a *dSpace Scalexio* simulation system in real time.

The simulation model works as follows: The initial instance is the environment block, which transmits data such as temperature, solar radiation, drive cycle and the number of passengers to the next instance. The train dynamics block then calculates the demanded traction force and the demanded train speed from the received signals. The demanded traction force and the resulting speed profile are transmitted to the EMU, which calculates the required electrical traction power and whose algorithms distribute it to the propulsion components according to the current operating strategy. The drive component models (fuel cell and battery) receive the demanded power respectively and report to the EMU whether the requested power can be provided or not (see Figure 2).

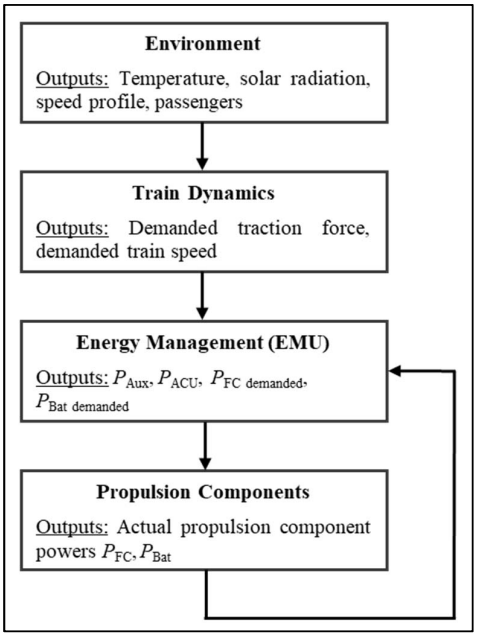

Figure 2: Overview of the functionality of the simulation model

B. Energy Management Unit (EMU)

The EMU performs the power management of the simulation model. The EMU calculates the demanded electrical power to move the train considering system boundaries and constraints of the components. Under consideration of the air conditioning unit and the auxiliary power unit, the EMU calculates total power demand P_{Demand} as follows:

$$P_{\text{Demand}} = P_{\text{Traction}} + P_{\text{Aux}} + P_{\text{ACU}} + P_{\text{Loss}} \quad (1)$$

$$P_{\text{Traction}} = [0.5\rho ACv^2 + fmg + ma + mgs + bmv] \cdot v \quad (2)$$

P_{Traction} is the electric power to fulfill the drive cycle requirements. P_{Aux} is the power demand of auxiliary consumers, e.g. on-board electronics. The average value of P_{Aux} is 30 kW. P_{ACU} is the power demand of the air conditioning unit. P_{ACU} depends on the solar radiation and the temperatures inside and outside of the vehicle. The average value of P_{ACU} is approximately 15 kW. P_{Loss} describes the losses of the power train (i.e. considering efficiencies of components such as DC-DC converters). Equation (2) calculates P_{Traction} with ρ as density of air; A as reference area; C as air resistance coefficient; v as velocity of the train; f is the rolling resistance coefficient; a represents the train acceleration; s is the slope; b is the coefficient related to the rail [10, 11].

C. Battery model

Prior to the simulation, we carried out measurements on the battery cell. Based on these measurements, the utilized battery model is parameterised to a previously defined equivalent circuit diagram. The resulting battery model includes diffusion elements for slow excitations and double-layer capacitances for fast excitations [12].

Figure 3 shows the performance of the simulated battery model in comparison to a validation cell measurement as the reference. The average percentage deviation amounts to 0.22 % and the root-mean-square error is 6.8 mV across the

measured range. Larger deviation of the voltage response can be observed with sharp current pulses. The battery cells of the pack will be operated between 2.05 V and 2.6 V. To guarantee the dynamic accuracy of the battery model for drive modes like braking or acceleration, the responsiveness of current ripples is displayed in the enlarged area of Figure 3.

For the optimization algorithms, a look-up table based model of the battery cell voltage V_{Cell} is used. The look-up tables were generated from real cell measurements and have the battery's SoC and the charge or discharge current I_{Cell} as input variables.

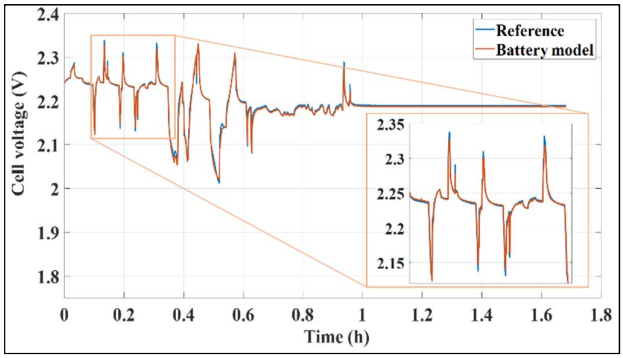

Figure 3: Comparison of the voltage response of the battery model with the measured voltage of the validation cell measurement (reference).

D. Fuel cell model

The fuel cell used in the simulation model represents a proton-exchange membrane fuel cell system. The performance and the fuel consumption of the fuel cell is modelled by look-up tables inside the simulation model. Measurement results from the test bench will serve as the basis for parameterization and validation of the simulation model.

E. Drive Cycle

The investigated driving cycle simulates a half-hour drive. After about 1400 s, the simulated train takes a short pause, followed by an acceleration and the speed peak in the cycle. The maximum acceleration is found in the beginning of the drive cycle between 0 s and 10 s with 1.045 m/s² (see Figure 4).

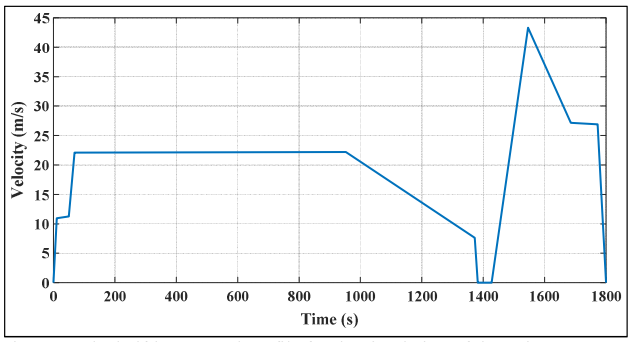

Figure 4: The half-hour speed profile for the simulation of the train.

III. Operation Strategies and Calculation Results for the Energy Management

The calculated power demand is distributed to the battery (P_{Bat}) and to the fuel cell (P_{FC}) and the optimization seeks an optimum distribution of P_{Demand}:

$$P_{Demand} = P_{Bat} + P_{FC} \quad (3)$$

Three strategies for the power distribution between the battery and the fuel cell have been examined. The following energy costs have been used as a basis for the optimization calculations [13, 14]:

- Hydrogen fuel price: 4.50 € / kg
- Battery energy price: ± 0.175 € / kWh

System boundaries and initial conditions for the battery and the fuel cell are:

$$-1000\ \text{kW} < P_{Bat} < 1000\ \text{kW} \quad (4)$$

$$50\ \text{kW} < P_{FC} < 200\ \text{kW} \quad (5)$$

$$SoC_{t=0} = 100\ \% \quad (6)$$

A. Rule-based strategy

An on-line rule-based strategy, which distributes the power demand according to the battery's SoC between the battery and the fuel cell, is implemented within the EMU [15]. In this strategy, the fuel cell is set to either run at an efficient rate covering the base load or charge the battery, while the battery serves as a buffer for dynamic load peaks (such as acceleration or recuperation). The rule-based strategy distributes the power according to the SoC of the battery system through a set of conditional statements at each iteration of the simulation. The EMU conducts the rule-based strategy on-line without any information of the drive cycle. The battery is charged if possible at a low SoC. Similarly, the battery is discharged if possible at a high SoC (see Figure 5). The rule-based strategy is set up in such a way, that it keeps the SoC of the battery within 40 and 60 percent as long as enough hydrogen can be provided to the fuel cell. The rule-based strategy does not optimize the fuel economy.

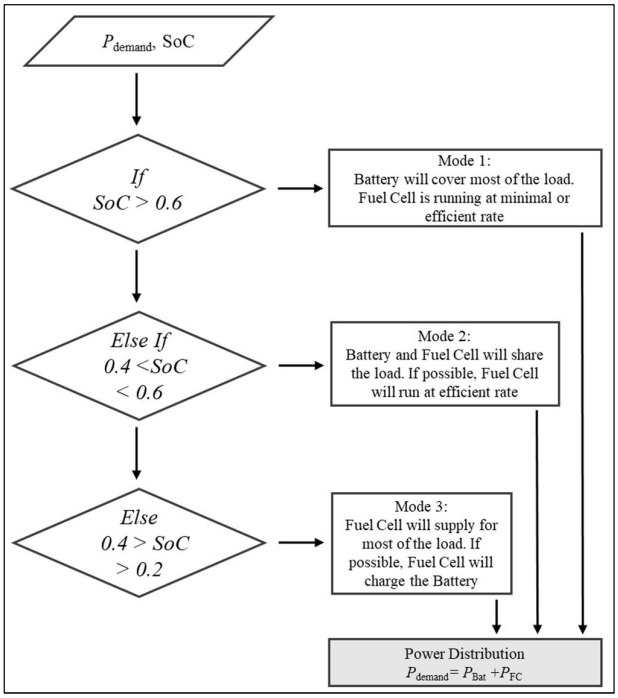

Figure 5: Sequential flow chart for the functional principle of the rule-based strategy within the EMU.

B. DP Optimization

The DP optimization approach seeks to optimize the costs function $c(\Delta t, SOC(t))$ of each state based on Bellman's principle of optimality [16]:

$$c(\Delta t, SOC(t)) = min(c(I_{Cell}, V_{Cell}, P_{Bat}, P_{FC}, m_H) + c_{new}) \quad (7)$$

The computational complexity increases exponentially with the number of state variables. Here, the SoC of the battery is defined as the state variable. Values, which can be assumed at time step t (Δt = 15 s) and at the states SoC are as follows:

- I_{Cell} which is known a-priori;
- V_{Cell} which is obtained by a look-up table from the SoC and I_{Cell};
- P_{Bat} is calculated by the multiplication of I_{Cell}, V_{Cell} with the number of cells n connected in series and in parallel (n_{series} and $n_{parallel}$);
- P_{FC} is calculated by the energy demand and with the help of equation 3;
- m_H – the hydrogen mass – which is obtained by a look-up table from P_{FC};
- c_{new} is the sum of energy costs, obtained from P_{Bat} and m_H.

The calculated optimal power distribution is stored and performed on the simulation model to ensure that the power distribution between the drive components works in the simulation environment.

C. QP Optimization

The QP approach minimises the sum of costs [17]. The battery power P_{Bat} is calculated as follows:

$$P_{Bat} = V_{Cell}(SoC, I_{Cell}) \cdot I_{Cell} \cdot n_{series} \cdot n_{parallel} \quad (8)$$

The fitted quadratic cell function V_{Cell} (SoC, I_{Cell}) is multiplied with the cell current I_{Cell} to obtain the cell power P_{Cell} and with the number of cells n connected in series and in parallel. The amount m_H of hydrogen is determined from a look-up table and equation 3. Hence, P_{FC} can be reformulated as

$$P_{FC} = P_{Demand} - V_{Cell}(SoC, I_{Cell}) \cdot I_{Cell} \cdot n_{series} \cdot n_{parallel}. \quad (9)$$

The algorithm minimizes the resulting costs of the quadratic problem. Analogous to the DP, the calculated optimal power distribution of the QP optimization is stored inside the simulation model and was performed on the simulation model.

D. Results of the Optimization

The results of the optimization are found in Table 1 and in Figure 6. The rule-based strategy was additionally benchmarked without the limitation for the minimum fuel cell power of 50 kW defined in equation 5. Nevertheless, the difference of costs between both rule-based strategies is marginal. The on-line rule based strategy is a resource-efficient alternative with practically no calculation time, since it is performed in real time. It is 36.25 % with the P_{FC} limitation or 35.56 % without the P_{FC} constraint respectively costlier than the QP optimization. The off-line QP strategy has the best performance in terms of costs and calculation time and serves as a reference for the difference of costs and the calculation time. The optimized costs of the DP strategy are 9.8 % higher and the calculation time is significantly higher with a factor of over 35. Therefore, the QP is the best operating strategy according to the current development status.

TABLE I. COMPARISON OF THE DIFFERENT POWER MANAGEMENT STRATEGIES

Energy Management Strategy	Total cost and resources of the drive cycle		
	Costs (€)	***Difference of costs (%)***	***Calculation time[a]***
On-line rule-basedrule-based Strategy	49.14	+ 35.56	0 s[b]
On-line rule-based Strategy with P_{FC} > 50 kW	49.39	+ 36.25	0 s[b]
Off-line DP with Δt = 15 s	39.81	+ 9.8	193.4 s
Off-line QP with Δt = 15 s	36.25	0	5.4 s

[a] The calculation was performed on a Windows machine with an i7 quad-core CPU.

[b] The simulation model computes the rule-based strategies in real time.

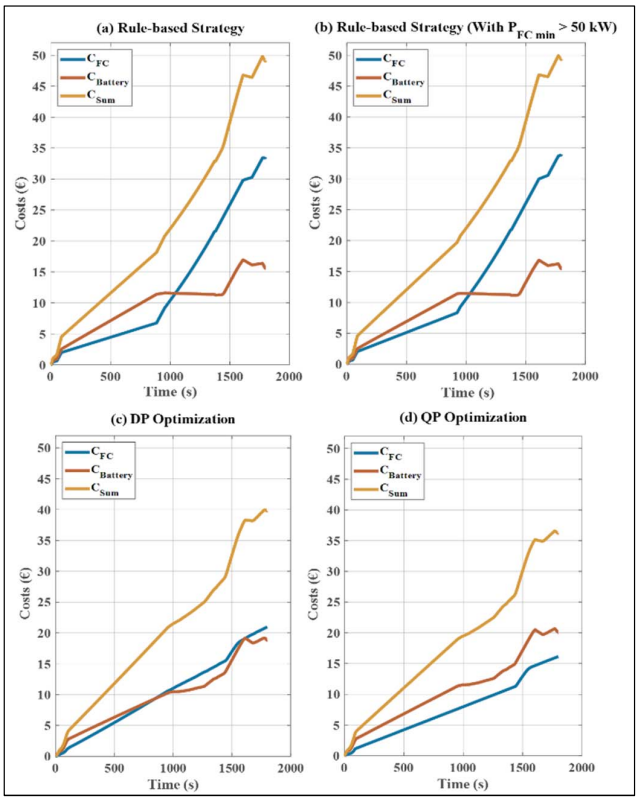

Figure 6: Graphs of the power distribution and the total costs for the drive cycle for different power management strategies; (a) Rule-based strategy without a minimum fuel cell power of 50 kW; (b) Rule-based strategy with the minimum fuel cell power of 50 kW; (c) DP Optimization; (d) QP Optimization.

IV. Conclusion

In this paper, the simulation model to perform energy management tasks on a HIL-test bench for a hybrid train is explained. It was shown that it is possible to model a large battery system with good accuracy for the energy management of the hybrid train. Additionally, different operation strategies for the energy and power management of the hybrid train were presented and compared. The operation strategies will also be tested and validated on the test bench.

In future research to this topic, the battery model will be tested and validated on the HIL test bench. This includes the aforementioned deviation with pulses. Additionally, more states for the optimization such as ageing of the battery and the fuel cell should be considered for future research. The stress caused by the drive cycle can be transformed into a monetary penalty by an ageing model. The ageing increases the cost of the driving cycle and reduces the performance of the propulsion components eventually. However, this will require extensive measurements of the battery and fuel cell as well as additional computing resources.

Acknowledgements

This work was kindly funded by the German Federal Ministry of Transport and Digital Infrastructure (BMVi) under the National Innovation Programme Hydrogen and Fuel Cell Technology (funding code 03B10502, project "X-EMU").

V. References

[1] European Commission Directorate-General for Research and Innovation Smart, Green and Integrated Transport, Ed., "Electrification of the Transport System,"

[2] SCI Verkehr GmbH, *New Study: Railway Electrification Continues to Grow in 2018: World market for railway electrification continues to grow, sustained investments in Europe and Asia lead to high current market volume as well as growth up to 2022.* [Online] Available: https://www.masstransitmag.com/rail/press-release/12408644/sci-verkehr-gmbh-new-study-railway-electrification-continues-to-grow-global-market-development-2018. Accessed on: Aug. 09 2019.

[3] European Commission, *Electrified railway lines.* [Online] Available: https://ec.europa.eu/transport/facts-fundings/scoreboard/compare/energy-union-innovation/share-electrified-railway_en#2016.

[4] P. Garcia, L. M. Fernandez, C. A. Garcia, and F. Jurado, "Energy Management System of Fuel-Cell-Battery Hybrid Tramway," *IEEE Trans. Ind. Electron.*, vol. 57, no. 12, pp. 4013–4023, 2010.

[5] W. Enang and C. Bannister, "Modelling and control of hybrid electric vehicles (A comprehensive review)," *Renewable and Sustainable Energy Reviews*, vol. 74, pp. 1210–1239, 2017.

[6] C. M. Martinez *et al.,* "Energy Management in Plug-in Hybrid Electric Vehicles: Recent Progress and a Connected Vehicles Perspective," *IEEE Trans. Veh. Technol.*, vol. 66, no. 6, pp. 4534–4549, 2017.

[7] M. F. M. Sabri, K. A. Danapalasingam, and M. F. Rahmat, "A review on hybrid electric vehicles architecture and energy management strategies," *Renewable and Sustainable Energy Reviews*, vol. 53, pp. 1433–1442, 2016.

[8] L. Serrao, S. Onori, and G. Rizzoni, "A Comparative Analysis of Energy Management Strategies for Hybrid Electric Vehicles," *J. Dyn. Sys., Meas., Control*, vol. 133, no. 3, p. 31012, 2011.

[9] X. Hu, N. Murgovski, L. M. Johannesson, and B. Egardt, "Optimal Dimensioning and Power Management of a Fuel Cell/Battery Hybrid Bus via Convex Programming," *IEEE/ASME Trans. Mechatron.*, vol. 20, no. 1, pp. 457–468, 2015.

[10] J. Ihme, *Schienenfahrzeugtechnik*. Wiesbaden: Springer Vieweg, 2016.

[11] de Doncker, Rik Wivina Anna, M. Niessen, H. Hoffmann, and G. Jacobs, "Electrical Design of a Novel Diesel-Electric Drivetrain for Suburban Trainsets using a Power Split Variator and Energy Storage System - Design and operation strategy of the electrical part of the energy storage system and variator drive," 2018.

[12] F. E. Hust, "Physico-Chemically Motivated Parameterization and Modelling of Real-Time Capable Lithium-Ion Battery Models - a Case Study on the Tesla Model S Battery,"

[13] S. Weidner *et al.,* "Feasibility study of large scale hydrogen power-to-gas applications and cost of the systems evolving with scaling up in Germany, Belgium and Iceland," *International Journal of Hydrogen Energy*, vol. 43, no. 33, pp. 15625–15638, 2018.

[14] German Association of Energy and Water Industries, "Strompreisanalyse Januar 2019," Berlin, Jan. 15 2019.

[15] H. Banvait, S. Anwar, and Y. Chen, "A rule-based energy management strategy for Plug-in Hybrid Electric Vehicle (PHEV)," in *A Rule-Based Energy Management Strategy for Plug-in Hybrid Electric Vehicle (PHEV)*, St. Louis, MO, USA, Jun. 2009 - Jun. 2009, pp. 3938–3943.

[16] R. Bellman, "The theory of dynamic programming," *Bull. Amer. Math. Soc.*, vol. 60, no. 6, pp. 503–515, https://projecteuclid.org:443/euclid.bams/1183519147, 1954.

[17] R. Fletcher, "Quadratic Programming," in *Practical Methods of Optimization*, R. Fletcher, Ed., Chichester, West Sussex England: John Wiley & Sons, Ltd, 2000, pp. 229–258.